Time-Slice Wavefield Decomposition

Max Holicki,Kees Wapenaar and Guy Drijkoningen, Delft University of Technology*

SUMMARY

We propose a novel acoustic decomposition operator for time slices, loosely based on conventional surface decomposition operators. The proposed operators hold for constant velocity models and require two 2D Fourier Transforms (one forward, one backward) per decomposed time slice per decomposition direction. We then demonstrate the capabilities of our operators on a constant velocity model and the Marmousi model. The decomposition results prove that we can decompose into up-, down-, left- and right-going waves for complex velocity media.

INTRODUCTION

Wavefield decomposition is a powerful seismic processing technique used in a plethora of processing steps ranging from ghost and multiple removal techniques to redatuming, imaging and inversion techniques. Historically, wavefield decomposition was applied to surface recordings, by for example Amundsen and Reitan (1995), to decompose wavefields entering and exiting surfaces. More recently, with the advancement of Reverse Time Migration (RTM) and Full Waveform Inversion (FWI), geoscientists became interested in decomposing wavefields everywhere inside a medium, instead of only on some surface. These configurations were simpler to decompose in the wavenumber frequency domain by decomposing in the direction of the wavenumber, however recording wavefields for all time steps everywhere came at significant computational cost.

We therefore propose a decomposition scheme that no longer decomposes after sufficient recording in time, but decomposes on time-slices, for constant velocity density media, and will demonstrate that it is applicable to more heterogeneous media. This is achieved by following a very similar approach as in Wapenaar and Berkhout (1989), but substituting for the frequency instead of the surface-normal wavenumber.

CONVENTIONAL DECOMPOSITION

With the advancements of RTM in the seismic industry as the tool for depth migration, migration noise became more and more of a problem. It can be shown that one can alleviate the problem by directionally decomposing wavefields, as done in Díaz and Sava (2015). Yoon and Marfurt (2006) had already developed a new RTM imaging condition based on decomposing acoustic wavefields based on their Poynting vector, an electromagnetic concept introduced by Poynting (1884), to improve imaging and reduce RTM noise. Poynting decomposition advanced as a powerful local decomposition technique that failed when wavefields interfered, as in the acoustic case it is simply the multiplication of the pressure wavefield p with the particle velocity in the decomposition direction of interest v. Since then Poynting RTM imaging has been further refined, by, for example, Chen and He (2014).

Alternatively, one can record the wavefield everywhere for all time samples, which comes at high storage costs. One can then decompose the waves into up- and down-going in the vertical wavenumber-frequency domain or left- and right-going in the horizontal wavenumber-frequency domain, as demonstrated by Hu and McMechan (1987). To get the up-going wavefield one mutes all terms for which the product of the vertical wavenumber and the frequency is negative.

However it was found, by Frasier (1970) among others, that recording the entire wavefield everywhere in time and space is not necessary to decompose it, as long as the recordings are multicomponent. By scaling the particle velocity along a surface in the direction of decomposition, which must be normal to the surface, in the wavenumber-frequency domain, it is possible to decompose the wavefield assuming constant velocity and density. Wapenaar and Grimbergen (1996) extended this to heterogeneous velocities by deriving approximate operators with limited lateral support. These operators however are hardly applicable to time-slices of wavefields. We also realized that most operators in the literature are in the ω-k_x or ω-k_z domain, the k_x-k_z, decomposition was missing. We will now fill this gap.

THEORY

To derive our acoustic decomposition operators we begin with the source free linearized equation of motion and continuity in Einstein's summation notation for homogeneous media in the space-time domain (Aki and Richards, 2002), more specifically the (x,z,t) domain, where in 2D x and z are the horizontal and vertical directions respectively and t is time:

$$\rho c^2 \partial_i v_i = -\partial_t p \tag{1a}$$

$$\rho \partial_t v_i = -\partial_i p \tag{1b}$$

where ∂ denotes derivatives in their subscript direction and Latin subscripts denote the two spatial dimensions. Here $v_i(x,z,t)$ is the particle velocity, $p(x,z,t)$ is the pressure, c is the homogeneous medium velocity and ρ is the homogeneous density. Transforming to the wavenumber-frequency domain (k_x,k_z,ω), where k_x and k_z are the horizontal and vertical wavenumber respectively and ω is the angular frequency, gives:

$$\rho c^2 k_i \tilde{V}_i = \omega \tilde{P} \tag{2a}$$

$$\omega \rho \tilde{V}_i = k_i \tilde{P} \tag{2b}$$

Capital letters denote temporally Fourier transformed data while $\sim$ hats indicate wavenumber transformed data.Transforming the single-depth-level decomposition relation (Wapenaar and Berkhout, 1989) from the (k_x,z,ω) domain to the (k_x,k_z,ω)

domain, we obtain the following

$$\begin{pmatrix}\tilde{P}^{\uparrow}\\ \tilde{P}^{\downarrow}\end{pmatrix}=\frac{1}{2}\begin{pmatrix}1 & -\frac{\omega\rho}{\kappa_z}\\ 1 & \frac{\omega\rho}{\kappa_z}\end{pmatrix}\begin{pmatrix}\tilde{P}\\ \tilde{V}_z\end{pmatrix} \tag{3a}$$

where the vertical Helmholtz operator κ_z is defined as:

$$\tilde{\kappa}_z^2 := \frac{\omega^2}{c^2}-k_x^2 \tag{3b}$$

We now make use of the dispersion relation:

$$\frac{\omega^2}{c^2}=k_i k_i \tag{4}$$

to substitute for κ_z and ω:

$$\tilde{\kappa}_z=|k_z| \tag{5}$$

$$\omega=c\sqrt{k_i k_i} \tag{6}$$

The square roots were chosen positive. This allows us to find:

$$\tilde{P}^{\uparrow}=\frac{1}{2}\left(\tilde{P}-\rho c\sqrt{\frac{k_i k_i}{k_z^2}}\tilde{V}_z\right) \tag{7a}$$

$$\tilde{P}^{\downarrow}=\frac{1}{2}\left(\tilde{P}+\rho c\sqrt{\frac{k_i k_i}{k_z^2}}\tilde{V}_z\right) \tag{7b}$$

The scale factor is now independent of ω, allowing us to transform back to the time domain easily:

$$\tilde{p}^{\uparrow}=\frac{1}{2}\left(\tilde{p}-\rho c\sqrt{\frac{k_i k_i}{k_z^2}}\tilde{v}_z\right) \tag{8a}$$

$$\tilde{p}^{\downarrow}=\frac{1}{2}\left(\tilde{p}+\rho c\sqrt{\frac{k_i k_i}{k_z^2}}\tilde{v}_z\right) \tag{8b}$$

Transforming back to the space domain we find:

$$p^{\uparrow}=\frac{1}{2}\left(p-\rho c\mathfrak{F}_{x,z}^{-1}\left\{\sqrt{1+\left(\frac{k_x}{k_z}\right)^2}\tilde{v}_z\right\}\right) \tag{9a}$$

$$p^{\downarrow}=\frac{1}{2}\left(p+\rho c\mathfrak{F}_{x,z}^{-1}\left\{\sqrt{1+\left(\frac{k_x}{k_z}\right)^2}\tilde{v}_z\right\}\right) \tag{9b}$$

Expressions for left-right decomposition may be found:

$$p^{\leftarrow}=\frac{1}{2}\left(p-\rho c\mathfrak{F}_{x,z}^{-1}\left\{\sqrt{1+\left(\frac{k_z}{k_x}\right)^2}\tilde{v}_x\right\}\right) \tag{10a}$$

$$p^{\rightarrow}=\frac{1}{2}\left(p+\rho c\mathfrak{F}_{x,z}^{-1}\left\{\sqrt{1+\left(\frac{k_z}{k_x}\right)^2}\tilde{v}_x\right\}\right) \tag{10b}$$

Similar relations can be found for decomposed velocity wavefields:

$$v_z^{\uparrow}=\frac{1}{2}\left(v_z-\frac{1}{\rho c}\mathfrak{F}_{x,z}^{-1}\left\{\sqrt{1+\left(\frac{k_x}{k_z}\right)^2}^{-1}\tilde{p}\right\}\right) \tag{11a}$$

$$v_z^{\downarrow}=\frac{1}{2}\left(v_z+\frac{1}{\rho c}\mathfrak{F}_{x,z}^{-1}\left\{\sqrt{1+\left(\frac{k_x}{k_z}\right)^2}^{-1}\tilde{p}\right\}\right) \tag{11b}$$

$$v_z^{\rightarrow}=\frac{k_z}{k_x}v_x^{\rightarrow} \tag{11c}$$

$$v_z^{\leftarrow}=\frac{k_z}{k_x}v_x^{\leftarrow} \tag{11d}$$

There are analogous expressions for theup- and down-ward propagating horizontal particle velocity v_x. Using the thus far derived decomposed pressures and particle velocities, we can now combine them to decompose our wavefields into quadrants. For example the up-right going pressure wavefield may be written in two ways as:

$$p^{\nearrow}=\frac{1}{2}\left(p^{\uparrow}+\rho c\mathfrak{F}_{x,z}^{-1}\left\{\sqrt{1+\left(\frac{k_z}{k_x}\right)^2}\tilde{v}_z^{\uparrow}\right\}\right) \tag{12a}$$

$$p^{\nearrow}=\frac{1}{2}\left(p^{\rightarrow}-\rho c\mathfrak{F}_{x,z}^{-1}\left\{\sqrt{1+\left(\frac{k_x}{k_z}\right)^2}\tilde{v}_x^{\rightarrow}\right\}\right) \tag{12b}$$

Analogs exist for quadrant particle velocity decomposition. To extend this to 3D, the square root term for the up-down decomposition has an additional $(k_y/k_z)^2$ term, this can be extended to other decomposition directions. We can now use these equations to decompose snapshots for homogeneous velocity-density models.

To decompose wavefields in more heterogeneous velocity models, we locally approximate the operation at each grid point by replacing the homogeneous velocity with the actual velocity of the gridpoint. Effectively stating that $c=c(x_m,z_n)$ in the neighborhood of the gridpoint (m,n). This yields very acceptable results as our second decomposition demonstrates.

NUMERICAL EXAMPLES

We will now discuss two constant density numerical models, a constant 1 km/s model and the Marmousi model (Brougois et al., 1990), to highlight the advantages and limitations of this decomposition method on grids over other decomposition techniques.

Constant velocity & density

Figure 1 shows a snapshot of an acoustic wavefield in a contant 1 km/s constant 1 g/cm model. The data were modeled using using a 2$^{\text{nd}}$ order finite difference acoustic scheme with a volume injection source at the center of the model, injecting a 60 Hz Ricker wavelet. Horizontal and vertical grid spacing were 1 m, the modeling time step was 0.5 ms, and the pressure and velocity grid were staggered with rigid boundaries.

In Figures 1b, 1c, and 1d, which show the decomposed fields, we see that there is some leakage of the wavefield. It should be noted that at earlier time steps, when the source is active, the leakage is stronger because the source is not properly taken into account by our decomposition scheme. The leakage, in Figure 1, is primarily due to the fact that the modeling grids are both staggered in time and space, we corrected for this in the space domain, but there is still a half time step difference between the two. To reduce edge artifacts the data were tapered at the edges of the model and for non-physical arrivals. There are also some low wavenumber spurious artifacts where the wavefields do not propagate in the decomposition direction.

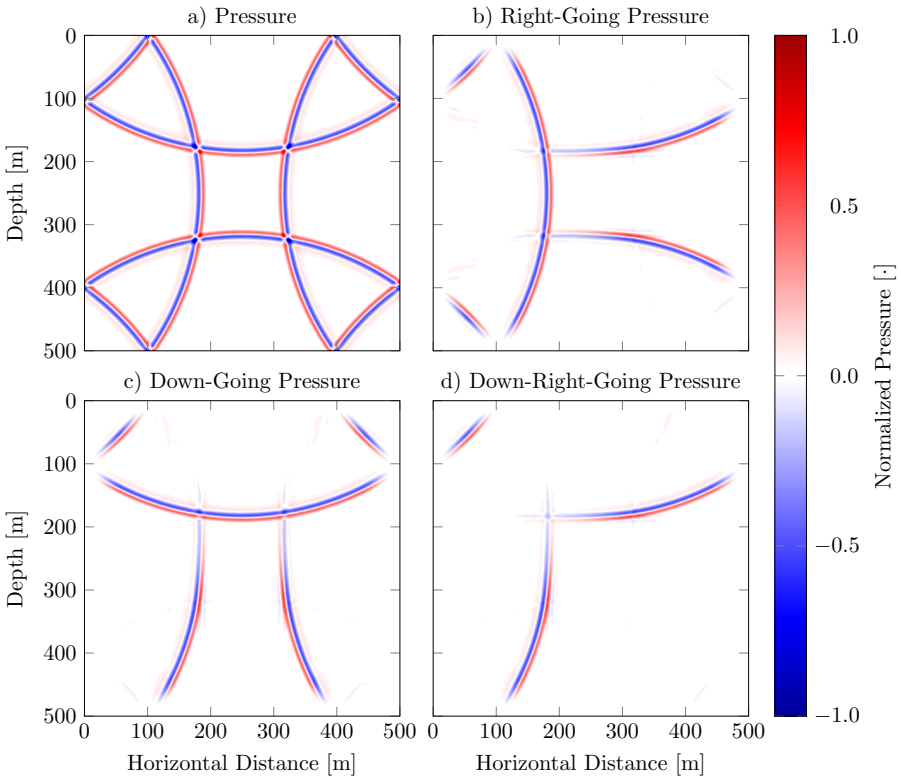

Figure 1: a) shows the full pressure wavefield for a constant density constant 1 km/s model, b) and c) show the right- and down-going pressure and d) shows the down-right-going pressure. Normalized to the maximum pressure in the time-slice.

Another point of interest is that, although we taper the edges to reduce low vertical wavenumber artifacts, rigid boundary reflections are taken into account without having to include them specifically in the equations.

Marmousi

Figure 2 shows a snapshot of an acoustic wavefield due to a source at the center of the Marmousi model. Figure 2a shows the total pressure wavefield, Figure 2b shows the rightward propagating pressure,Figure 2c shows the upward propagating pressure and Figure 2d shows the model. The data were normalized to the maximum pressure in each time slice. The data were modeled in the same fashion as the constant velocity model but the horizontal and vertical grid spacing were 4 m, the peak frequency of the Ricker wavelet was 20 Hz and the modeling time step was 0.2 ms.

We see that we are able to directionally decompose the wavefields very nicely and they look much cleaner when compared to the total pressure. There is no visible leakage of the downward propagating wavefield in Figure 2c. In the lower left or right corners in Figure 2c, one can see that we are able to accurately decompose interfering wavefields, something that is not possible for Poynting decomposition (Yoon and Marfurt, 2006). We note that errors due to complex velocity models are not directly apparent, which is surprising as the expression were derived assuming constant velocity. We can see the same features in the right-going wavefield in Figure 2b.

At early time steps we found that the upward propagating wavefield nicely separates from the downward propagating wavefield at interfaces. This kind of decomposition directly at interfaces is very difficult for the previously discussed conventional decomposition along depth levels.

COMPUTATIONAL IMPLICATIONS

This decomposition technique allows us to decompose our wavefields on time-slices, common in RTM or FWI. Previously one had to accept the limitations of Poynting decomposition if one wanted to decompose on a snapshot, or one had to record the modeled wavefield everywhere for all time slices before decomposing at the end, a computationaly very expensive task.

Decomposition on time-slices alleviate the above, however, care should be taken in the numerical implementation of the decomposition. The edges of the snapshots should be tapered to avoid wrap-around effects due to operations in the wavenumber domain; padding the model before transforming also helps. Poles arise in the square root operators when the wavenumber in the decomposition direction tend to zero. These can be approximated via the zero-wavenumber terms from the directions orthogonal to the decomposition direction. The scale factor of the zero wavenumber component is always 1. A similar approach should be taken when converting one velocity component to another.

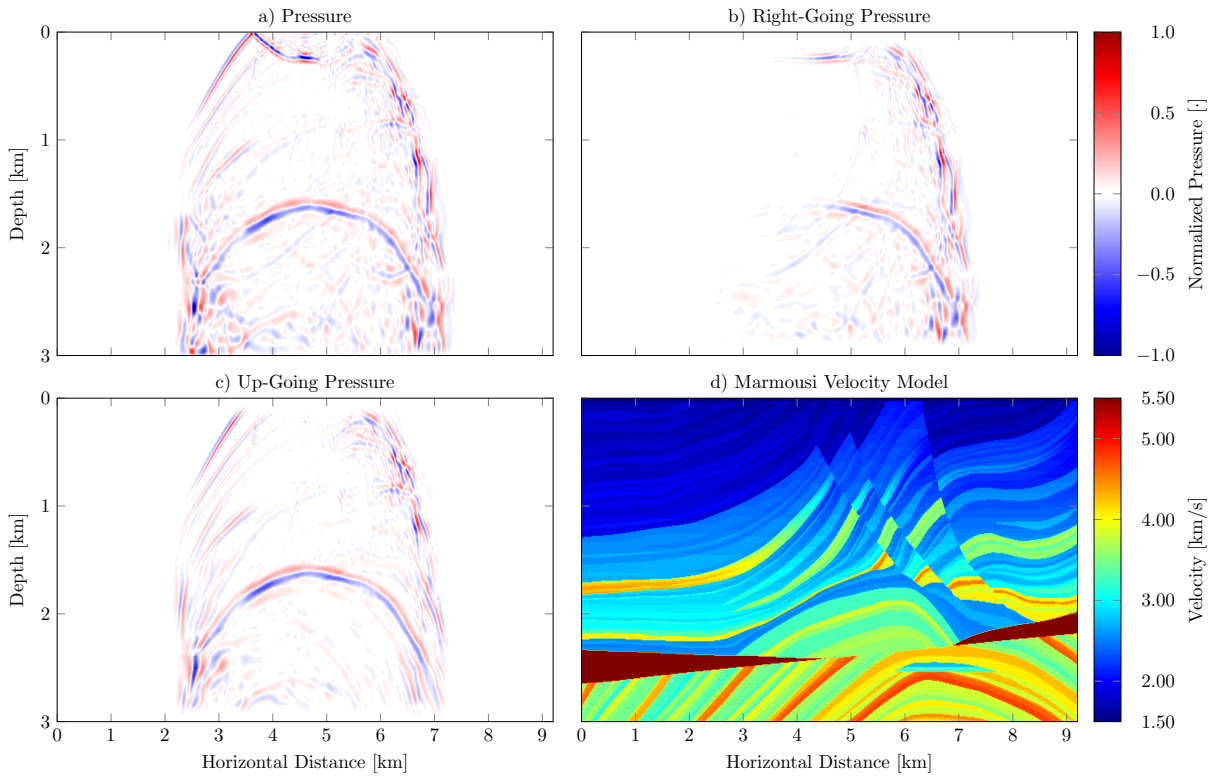

Figure 2: a) shows the pressure wavefield for the velocity model in d), b) and c) show the right- and up-going pressure wavefields. Normalized to the maximum pressure in the time-slice.

Care must also be taken when sources are active. The derived expressions are for the source free case. The expressions can be extended to include source terms, or one only decomposes when the time-slice is source free. The errors associated with the source may be large and overprint the decomposition.

CONCLUSIONS

We have derived n acoustica time-slice decomposition scheme for homogeneous velocity media, based on similar operators to those for single level decomposition, and approximated these to more complex velocity models. The decomposition scales the particle velocity in the direction of decomposition in the wavenumber domain to the pressure. This now allows us to decompose wavefields efficiently on time-slices without suffering from artifacts like in the faster Poynting decomposition. This technique could prove very useful for RTM and FWI where wavefield decomposition is growing in importance. It may also be possible to use the decomposition to implement absorbing boundaries for finite difference or finite element modeling schemes. This may be achieved by subtracting the wavefield propagating back into the model from the wavefield propagating out of the model in a boundary region at the edge of the model.

ACKNOWLEDGMENTS

We wish to thank Niels Grobbe, Joost van der Neut, Jan Thorbecke and Carlos Almagro Vidal, for their constructive feedback in the development of this theory.